



Kent Academic Repository

Wen, Le-Hu, Gao, Steven, Mao, Chun-Xu, Luo, Qi, Hu, Wei, Yin, Yingzeng and Yang, Xuexia (2018) *A Wideband Dual-Polarized Antenna Using Shorted Dipoles*. *IEEE Access*, 6 . pp. 39725-39733.

Downloaded from

<https://kar.kent.ac.uk/68247/> The University of Kent's Academic Repository KAR

The version of record is available from

<https://doi.org/10.1109/ACCESS.2018.2855425>

This document version

Publisher pdf

DOI for this version

Licence for this version

CC BY (Attribution)

Additional information

Versions of research works

Versions of Record

If this version is the version of record, it is the same as the published version available on the publisher's web site. Cite as the published version.

Author Accepted Manuscripts

If this document is identified as the Author Accepted Manuscript it is the version after peer review but before type setting, copy editing or publisher branding. Cite as Surname, Initial. (Year) 'Title of article'. To be published in *Title of Journal* , Volume and issue numbers [peer-reviewed accepted version]. Available at: DOI or URL (Accessed: date).

Enquiries

If you have questions about this document contact ResearchSupport@kent.ac.uk. Please include the URL of the record in KAR. If you believe that your, or a third party's rights have been compromised through this document please see our [Take Down policy](https://www.kent.ac.uk/guides/kar-the-kent-academic-repository#policies) (available from <https://www.kent.ac.uk/guides/kar-the-kent-academic-repository#policies>).

Received May 28, 2018, accepted July 2, 2018, date of publication July 12, 2018, date of current version August 7, 2018.

Digital Object Identifier 10.1109/ACCESS.2018.2855425

A Wideband Dual-Polarized Antenna Using Shorted Dipoles

LE-HU WEN¹, STEVEN GAO¹, (Senior Member, IEEE), CHUN-XU MAO²,
QI LUO¹, (Member, IEEE), WEI HU³, (Member, IEEE),
YINGZENG YIN³, (Member, IEEE), AND
XUOXIA YANG⁴, (Senior Member, IEEE)

¹School of Engineering and Digital Arts, University of Kent, Canterbury CT2 7NT, U.K.

²School of Electrical Engineering and Computer Science, The Pennsylvania State University, PA 16801, USA

³National Key Laboratory of Antennas and Microwave Technology, Xidian University, Xi'an 710071, China

⁴School of Communication and Information Engineering, Shanghai University, Shanghai 200444, China

Corresponding author: Le-Hu Wen (lw347@kent.ac.uk)

This work was supported in part by EPSRC under Grant EP/N032497/1 and in part by the Scholarship from the China Scholarship Council under Grant 201706960013.

ABSTRACT A novel design method of a wideband dual-polarized antenna is presented by using shorted dipoles, integrated baluns, and crossed feed lines. Simulation and equivalent circuit analysis of the antenna are given. To validate the design method, an antenna prototype is designed, optimized, fabricated, and measured. Measured results verify that the proposed antenna has an impedance bandwidth of 74.5% (from 1.69 to 3.7 GHz) for VSWR < 1.5 at both ports, and the isolation between the two ports is over 30 dB. Stable gain of 8–8.7 dBi and half-power beamwidth (HPBW) of 65°–70° are obtained for 2G/3G/4G base station frequency bands (1.7–2.7 GHz). Compared to the other reported dual-polarized dipole antennas, the presented antenna achieves wide impedance bandwidth, high port isolation, stable antenna gain, and HPBW with a simple structure and compact size.

INDEX TERMS Balun, base station, dual-polarized antenna, shorted dipoles, wideband antenna.

I. INTRODUCTION

With the rapid development of wireless communication systems, dual-polarized antennas are widely adopted owing to their advantages of reducing the multi-path fading and increasing the channel capacity [1]. Dual-polarized antennas have been widely applied in radars, satellites and mobile communication base stations. These systems usually require dual-polarized antennas with wide impedance bandwidth and high port isolation. Antennas for mobile communication base stations have some additional requirements, such as the stable antenna gain and HPBW over the frequency band of interest. With the emerging of the new wireless systems such as the fifth generation (5G) wireless communication system and others, it is important to investigate novel designs of high-performance antennas with dual-polarization, wide bandwidth, stable antenna gain and HPBW performance and compact size [2].

Many techniques for designing dual-polarized antennas have been reported. One conventional technique is to use microstrip patch antennas. Because of the orthogonal resonant modes (TM₀₁ and TM₁₀) on the patch, it is easy to

obtain high port isolation and high cross polarization discrimination (XPD). By using the multi-layer printed circuit board (PCB) technology and the aperture-coupling method, low profile dual-polarized antennas are reported in [3] and [4]. Other feed methods such as direct probe feed [5], [6], or proximity coupling [7]–[9] are also presented. Recently, wideband and dual-band dual-polarized filtering antennas with enhanced frequency selectivity are reported in [10] and [11]. These techniques enable the dual-polarized patch antennas to achieve an improved impedance bandwidth and high isolation better than 30 dB. However, the bandwidth of both impedance matching and high isolation is usually not wide enough to cover the frequency bands for 2G/3G/4G base station applications.

Dipoles are commonly used for dual-polarized antennas. A dual-polarized dipole antenna can be fed by either using coaxial cables [12]–[16], or printed baluns [17]–[19] for each linear polarization. A dual-polarized antenna using four folded dipoles is proposed [15]. This antenna has a stable radiation pattern and high cross polarization discrimination. However, its bandwidth is only 27.8%

for $SWR < 1.5$ (1.7-2.25 GHz). In [20], a dual-polarized antenna with stable gain and HPBW is presented, however, it requires four parasitic loop elements and a rectangular cavity-shaped reflector to realize stable radiation. Magneto-electric dipoles (MEDs) provide another method to design dual-polarized antennas [21]–[23]. Recently developed dual-polarized MED [23] utilizes dual open-ended slots for excitation. The measured overlapped impedance bandwidth of the antenna is 51.7% (with $SWR < 2$) for the two ports. Dual-polarized antennas for ultra-wideband (UWB) application are also reported in [24]–[26]. In [24], a square patch and four capacitive coupled feeds are utilized to enhance the impedance bandwidth, but a large cavity is required to reduce the backward radiation. Based on the tapered slot and the balun, antennas in [25] and [26] are realized for UWB application. Although these designs can obtain dual-polarization over a wide frequency band, the gain and HPBW of these antennas are unstable and cannot meet the requirements of the base station applications.

In this paper, a novel wideband $\pm 45^\circ$ dual-polarized antenna using four printed shorted dipoles is proposed. The four printed dipoles are symmetrically shorted in the center of the PCB and excited by two crossed feed lines. Compared to the traditional dual-polarized antennas, the proposed antenna has the three important advantages by using the baluns and shorted dipoles. Firstly, thanks to the integrated baluns, the proposed antenna achieves an improved impedance bandwidth of 74.5% (1.69-3.7 GHz) for $VSWR < 1.5$. Secondly, the isolation of two ports is higher than 30 dB over the whole antenna impedance bandwidth because of crossed feed configuration. Thirdly, with the configuration of two pairs of parallel shorted dipoles, a stable gain of 8.0-8.7 dBi and a stable HPBW of $65\text{-}70^\circ$ for 2G/3G/4G base stations are obtained without using any parasitic elements and modifying the reflector. In addition, the proposed antenna has a simple structure and compact size. Because of the wideband impedance bandwidth and good unidirectional radiation property, the proposed antenna is potentially useful for future 5G base stations, radars, satellites and other wireless systems.

II. ANTENNA CONFIGURATION

The configuration of the antenna is shown in Fig. 1. As shown in Fig. 1 (a), the antenna is composed of a PCB etched with the radiator and the feed lines, two 50 Ω RF coaxial cables, and a square reflector. On the bottom layer of the PCB, two pairs of shorted dipoles and four central shorted coplanar strip lines which operate as the baluns are printed. The top layer consists of two crossed feed lines, which are used to feed the power from the baluns to the radiator. The radiator and feed lines are printed on a low-cost substrate of Rogers 4003C, with ϵ_r of 3.55 and thickness of 0.813 mm.

The geometry parameters of the bottom layer radiator and top layer feed lines are shown in Fig. 1 (b) and Fig. 1 (c). The detailed dimensions are listed in Table 1. There are two circular slots around the center of the radiator on the bottom layer, which are used to solder the outer conductor of the

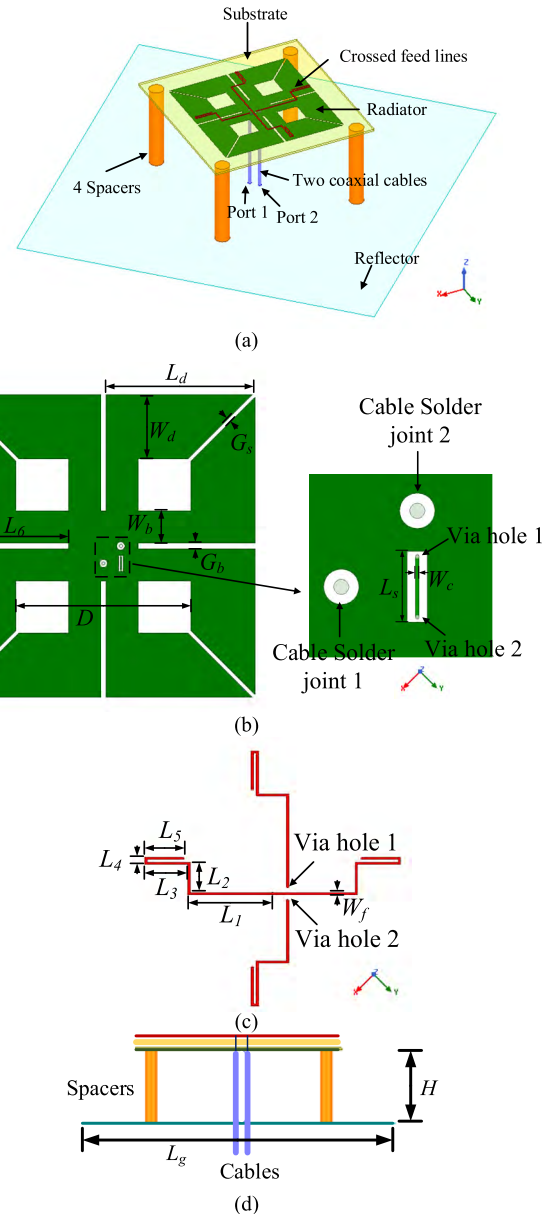


FIGURE 1. The configuration of the proposed antenna. (a) Isometric view of the antenna. (b) Bottom layer of the antenna substrate. (c) Top layer of the antenna substrate. (d) Side view of the antenna.

TABLE 1. Dimensions of the proposed antenna (mm).

W_b	W_c	W_d	W_f	L_s	L_1	L_2	L_3	L_4
5.5	0.15	11	0.4	2.8	16.5	6	8.5	1
L_5	L_6	L_d	G_b	G_s	D	L_g	H	
7.5	20	25	1	0.7	30	150	35	

two 50 Ω coaxial cables. Two crossed feed lines on the top layer are soldered to the inner conductor of the coaxial cables. There is a rectangular slot close to the two circular slots, which is utilized to avoid the intersection of two crossed feed lines. It should be noted that the vertical feed line is connected by two via holes and a narrow feed line on the

bottom layer. Its detailed configuration is zoomed in the right of Fig. 1 (b). Fig. 1 (d) shows the side view of the proposed antenna. The height of the radiator to the reflector is selected to 35 mm, which is about $\lambda_0/4$, where λ_0 is the free space wavelength at 2.2 GHz. The proposed antenna is designed for $\pm 45^\circ$ polarization as shown in the reference coordinate system in Fig. 1.

III. WORKING MECHANISM

A. IMPEDANCE MATCHING

To investigate the wideband characteristic of the proposed antenna, the equivalent circuit of the antenna is shown in Fig. 2. Due to the symmetry of the antenna structure, only one polarization is analyzed. As shown in the figure, port 1 is connected by a coaxial cable with the characteristic impedance of $Z_0 = 50\Omega$. Then it is connected by two identical baluns, which transform the input impedance of dipoles (Z_A) to the characteristic impedance of the microstrip feed lines (Z_1). For the design of the balun, the characteristic impedance of the crossed feed line (Z_1) is designed as 100Ω to match the high impedance of the coplanar strip line (Z_s). In addition, the parallel configuration of two 100Ω feed lines is also designed to match the 50Ω coaxial cable. The characteristic impedance and the length of the shorted coplanar strip line are Z_s and L_6 . The characteristic impedance of the open stub is Z_1 , with the length of $L_0 = L_2/2 + L_3 + L_4 + L_5$.

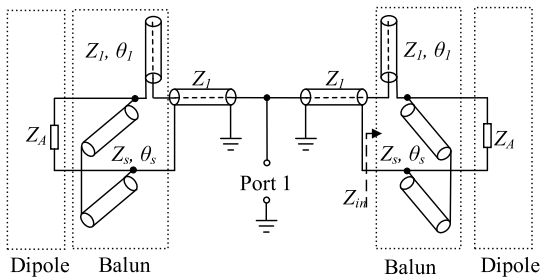


FIGURE 2. Equivalent circuit of the proposed antenna for one polarization.

According to the equivalent circuit in Fig. 2, the input impedance of the wideband balun Z_{in} can be expressed as [27]:

$$Z_{in} = -jZ_1 \cot\theta_1 + jZ_s \tan\theta_s || Z_A \quad (1)$$

where θ_1 is the electrical length of open stub, and θ_s is the electrical length of the shorted coplanar strip line. When the input impedance (Z_{in}) equals the characteristic impedance (Z_1), the proposed antenna obtains impedance matching. Assuming $Z_A = Z_s$, the equation (1) can be simplified to:

$$Z_{in} = Z_s \sin^2\theta_s + jZ_s \sin\theta_s \cos\theta_s - jZ_1 \cot\theta_1 \quad (2)$$

Assuming that the electrical length of open microstrip stub equals the electrical length of coplanar strip line:

$$\theta_s = \theta_1 = \theta \quad (3)$$

Then, considering the configuration of the proposed antenna, the conditions for equation (2) are: $Z_s = Z_A = 120\Omega$, and $Z_1 = 100\Omega$. Then the solutions for θ are

$$\begin{cases} \theta_0 = 90^\circ \\ \theta_1 = 65.91^\circ \\ \theta_2 = 114.09^\circ \end{cases} \quad (4)$$

The curves of the input impedance Z_{in} for the above conditions are shown in Fig. 3. It is observed that when $\theta_0 = 90^\circ$, $Z_{in} = 120\Omega$, and when $\theta_1 = 65.91^\circ$ and $\theta_2 = 114.09^\circ$, $Z_{in} = 100\Omega$, the balun transforms the antenna input impedance Z_A (120Ω) to Z_1 (100Ω). The image part has three zeroes, and θ_1 and θ_2 are symmetrical to θ_0 .

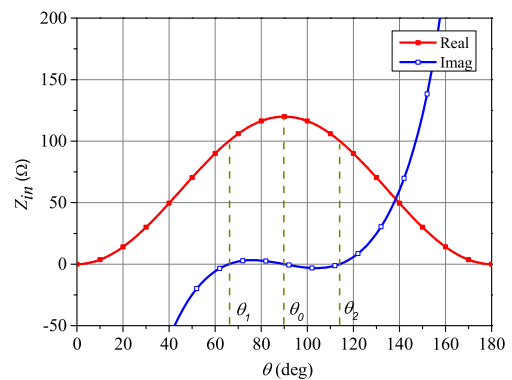


FIGURE 3. Input impedance of Z_{in} for equation (2).

Therefore, a wide impedance bandwidth can be obtained for the proposed antenna by integrating the shorted dipoles and baluns. Fig. 4 shows the simulated input impedance from the antenna port 1. All the simulation works in paper are obtained by 3D electromagnetic simulation software, ANSYS HFSS 2017. It is can be seen that the proposed antenna has multi-resonance characteristic. Within the interested frequency band from 1.5 GHz to 4 GHz, the imaginary part of the input impedance has six zeroes, and the real part maintains stable around 50Ω .

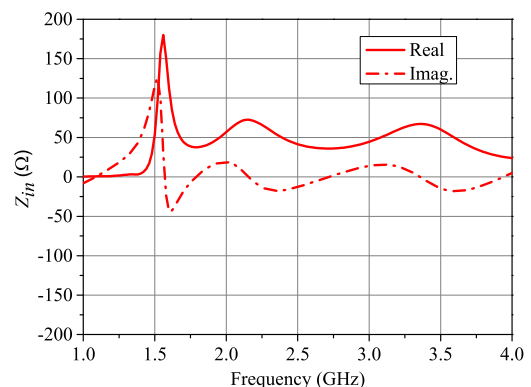


FIGURE 4. Simulated input impedance of antenna port 1.

To analyze the effect of wideband baluns on the impedance matching for the proposed antenna, parametric studies of

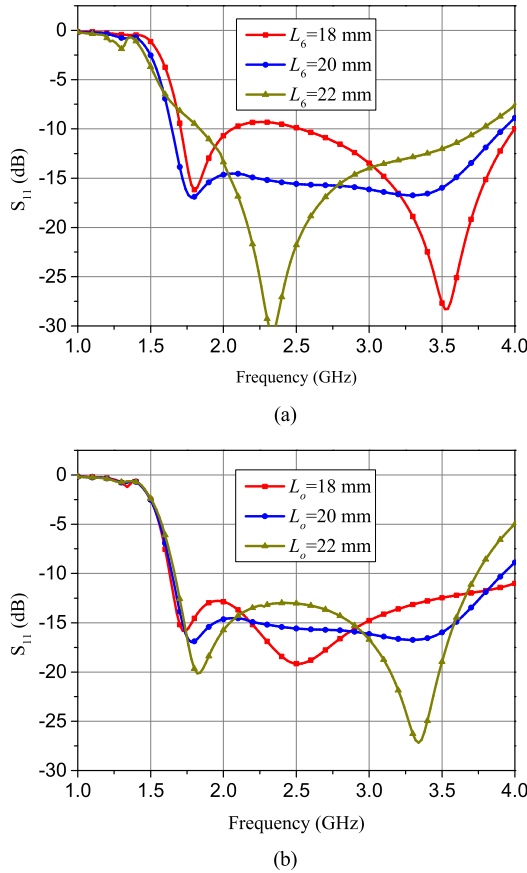


FIGURE 5. Simulated S_{11} with different length of (a) shorted coplanar strip line L_6 and (b) open stub L_o .

L_6 and L_o ($L_o = L_2/2 + L_3 + L_4 + L_5$) are performed. Fig. 5 shows the simulated S_{11} varies with different length of the shorted strip line and different length of open stub. It can be seen that when $L_6 = 18$ mm, there are two reflection zeros within the interest frequency band. However, the magnitude of the reflection coefficient is higher at about 2.2 GHz. For $L_6 = 22$ mm, the magnitude of the reflection coefficient at the center frequency is higher than -15 dB, but the bandwidth is narrower. As a trade-off, $L_6 = 22$ mm is selected, as the antenna has a flatter reflection response with three reflection zeroes. In Fig. 5 (b), when $L_o = 18$ mm, wider impedance bandwidth is obtained with a little higher reflection magnitude than $L_o = 20$ mm. But when L_o increases to 22 mm, the reflection zero in the center frequency band is disappeared with a little higher reflection magnitude. As shown, the baluns in this design play an important role on the impedance bandwidth for the proposed antenna.

It should be noted that the feed line for port 2 is a little different from port 1 because of the via holes connection in Fig. 1. Via holes can introduce additional parasitic inductances and the surrounding copper can introduce parasitic capacitance to the feed line. Accordingly, the deterioration of the input impedance at port 2 needs to be compensated

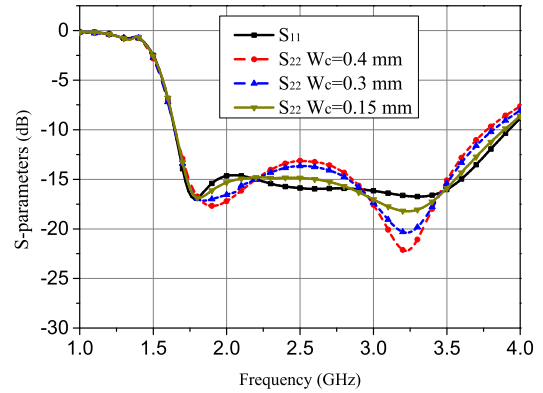


FIGURE 6. Simulated S_{22} with different width of connecting line (W_c).

by changing the width of the connecting line (W_c) on the bottom layer. As shown in Fig. 6, when W_c has the same width as the other feed line ($W_c = 0.4$ mm) at port 1, the reflection magnitude at the center frequency is deteriorated. When the W_c is decreased from 0.4 mm to 0.15 mm, almost the same reflection response is obtained for S_{22} compared to the S_{11} , and the deterioration is compensated by changing the width of the connecting line.

B. ANTENNA DESIGN

To explain the design approach better, the design flow of the proposed dual-polarized antenna is illustrated in Fig. 7. Antenna 1 is the simple four printed dipoles, two parallel dipoles are excited with same magnitude and phase for each polarization respectively. Antenna 2 is the four dipoles shorted in the center by coplanar strip lines. Both Antenna 1 and Antenna 2 are excited with ideal lumped ports in the simulation. Antenna 3 is the proposed antenna without the open stub. Instead, four conducting via holes are inserted

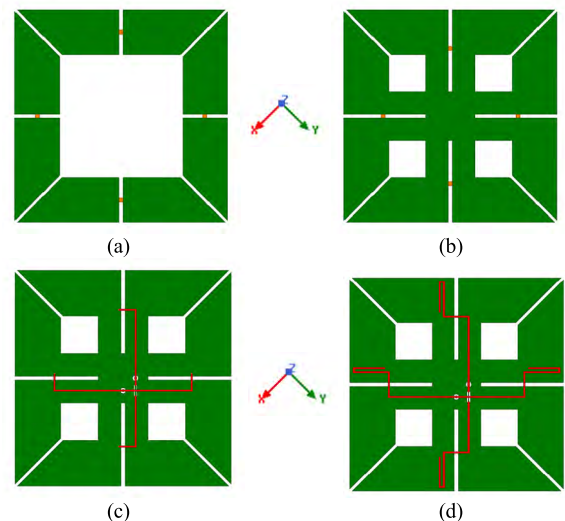


FIGURE 7. Design flow of the proposed dual-polarized antenna. (a) Antenna 1. (b) Antenna 2. (c) Antenna 3. (d) Antenna 4.

to feed the four dipole pairs. Antenna 4 is the proposed wideband dual-polarized antenna.

The simulated reflection coefficients of the four antennas are shown in Fig. 8. As can be seen, Antenna 1 shows a poor reflection coefficient. After incorporating the shorted strip lines, the reflection coefficient for Antenna 2 is even worse. However, the first reflection zero shifts to the lower frequency compared to Antenna 1. As the crossed feed lines are inserted into Antenna 3, the reflection coefficient gets much better and becomes lower than -10 dB. This improvement is mainly attributed to the contribution of the baluns, even if without the open stub. With the open stubs incorporated into the baluns for the proposed design (Antenna 4), the first reflection zero moves to even lower frequency, and the third reflection zero appears in the frequency band of interest. The simulated impedance bandwidth for S_{11} lower than -14 dB is increased from 1.7 GHz to 3.6 GHz.

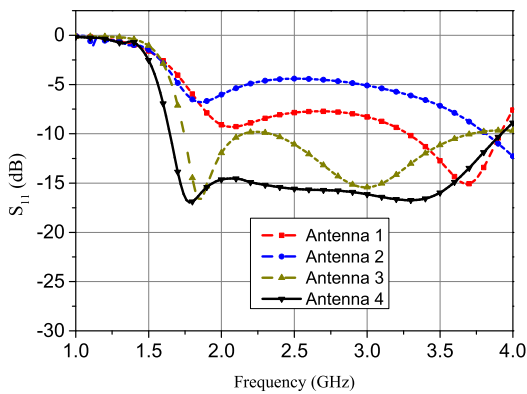


FIGURE 8. Simulated S_{11} for the evolution antennas.

To illustrate the working mechanism for the $\pm 45^\circ$ polarization, the current distribution of the proposed dual-polarized antenna at 2.5 GHz is shown in Fig. 9, and the auxiliary arrows are also added in the figure. It should be noted that, when port 1 is excited, $+45^\circ$ polarization is realized in the reference coordinate system. Correspondingly, -45° polarization is realized by exciting the antenna port 2. Solid arrows in the figure represent the current direction for

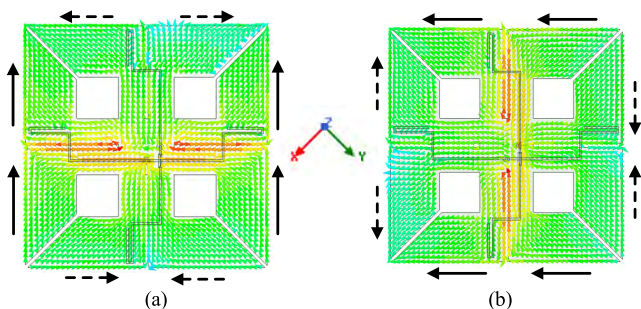
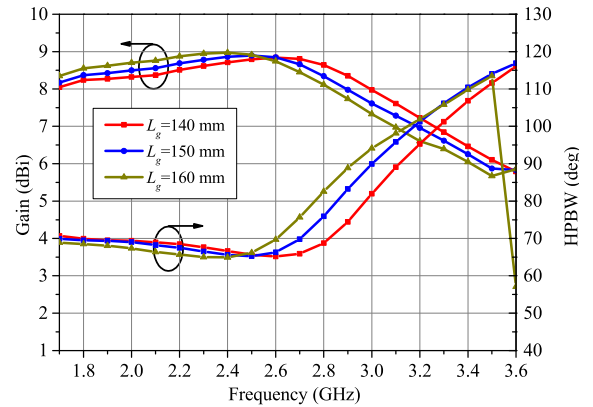
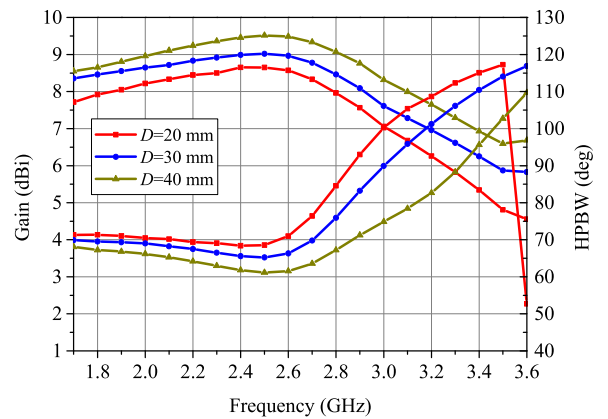


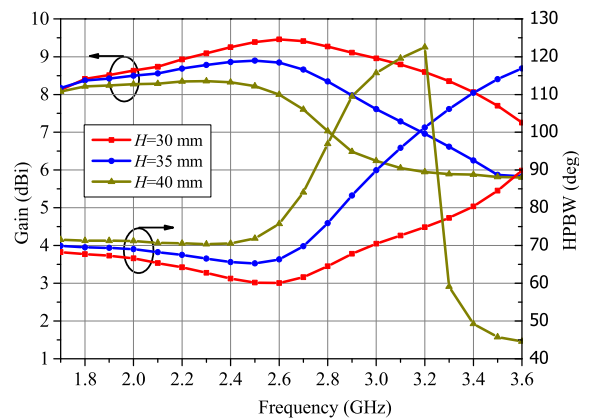
FIGURE 9. Current distribution for the proposed dual-polarized antenna at 2.5 GHz. (a) Port 1 is excited. (b) Port 2 is excited.



(a)



(b)



(c)

FIGURE 10. Study on the antenna gain and HPBW. (a) Length of the reflector (L_g). (b) The distance between the shorted dipoles (D). (c) Height between the radiator and reflector (H).

the co-polarization, whereas the dash arrow line represents the current direction for the cross-polarization.

In Fig. 9 (a), two parallel vertical dipoles are fed by the baluns for $+45^\circ$ polarization. Strong current distribution can be observed on the surface of the horizontal coplanar strip lines and the parallel vertical dipoles. Both the vertical dipoles are of the same current direction. For the horizontal dipole, inverse current distribution is induced on the two arms of the dipole. Furthermore, the common-mode current

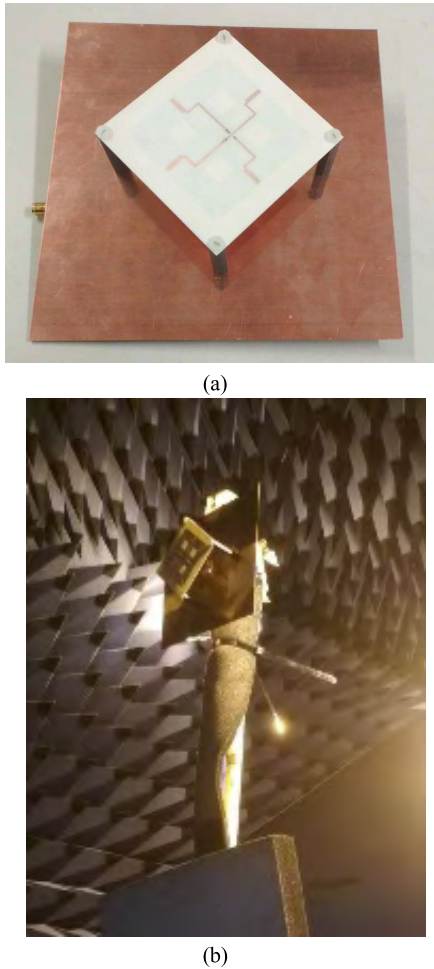


FIGURE 11. Prototype of the fabricated dual-polarized antenna. (a) Photograph of the proposed antenna. (b) Antenna under measurement in the anechoic chamber.

can be seen along the vertical coplanar strip lines, which means that good isolation and cross polarization can be obtained for the proposed antenna. Owing to the symmetry of the antenna radiator, the similar current distribution can be observed in Fig. 9 (b) when port 2 is excited. Thus, a same result can be obtained for the -45° polarization. Both the performances of high isolation and cross polarization are validated by the simulated and measured results in Section IV.

C. GAIN AND HPBW

To get a stable radiation characteristic for base station applications, different antenna parameters are studied. Parametric study shows that the parameters of the length of the square reflector (L_g), its distance to the radiator (H), and the distance between the two dipoles (D) have serious effects on the antenna radiation performances of gain and HPBW.

As shown in Fig. 10 (a), when the size of reflector (L_g) increases, the HPBW bandwidth for $60\text{-}70^\circ$ becomes narrow,

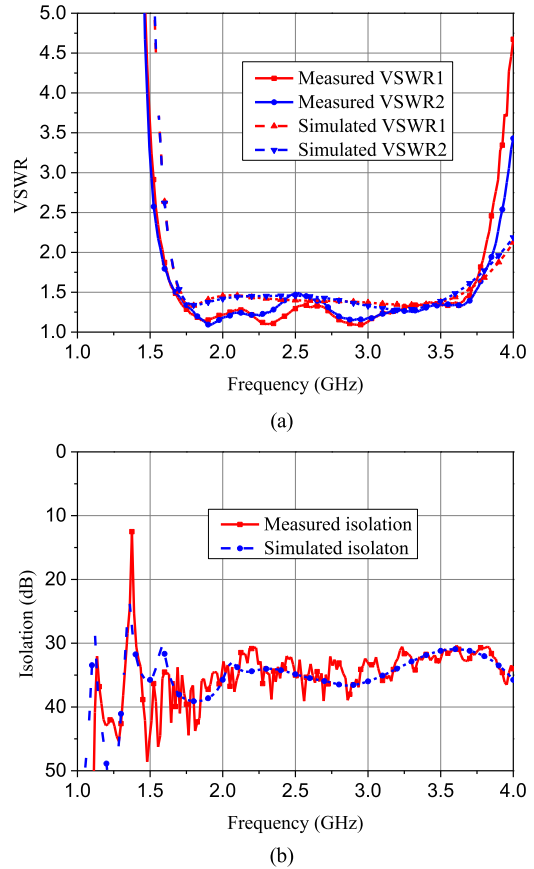


FIGURE 12. Measured and simulated (a) VSWR and (b) isolation of the proposed antenna.

and the gain for the lower band increases, but the gain of upper band decreases. As a whole, the bandwidth of gain and HPBW moves to the lower frequency with the increase of size of square reflector.

In Fig. 10 (b), with the distance between the two dipoles (D) increased, the HPBW bandwidth is improved and the gain increases due to the effect of array factor because of the dual-dipole configuration. The distance D provide another method to stabilize the antenna radiation property, which is different from the traditional dual-polarized cross dipole antennas.

The height (H) has a more significant effect on the antenna gain and HPBW. As shown in Fig. 10 (c), when $H = 30$ mm, the largest HPBW bandwidth is achieved, while the gain of the antenna rises and varies greatly. However, when H increases to 40 mm, due to the effect of the ground image of the antenna radiator, antenna beam is split into two beams, so the HPBW is sharply narrowed and the gain is decreased as the increase of the frequency.

Therefore, based on the antenna parametric study, parameters of L_g , D , and H are chosen to be $L_g = 150$ mm, $D = 30$ mm and $H = 35$ mm as a trade-off for the radiation requirements of the base station frequency band.

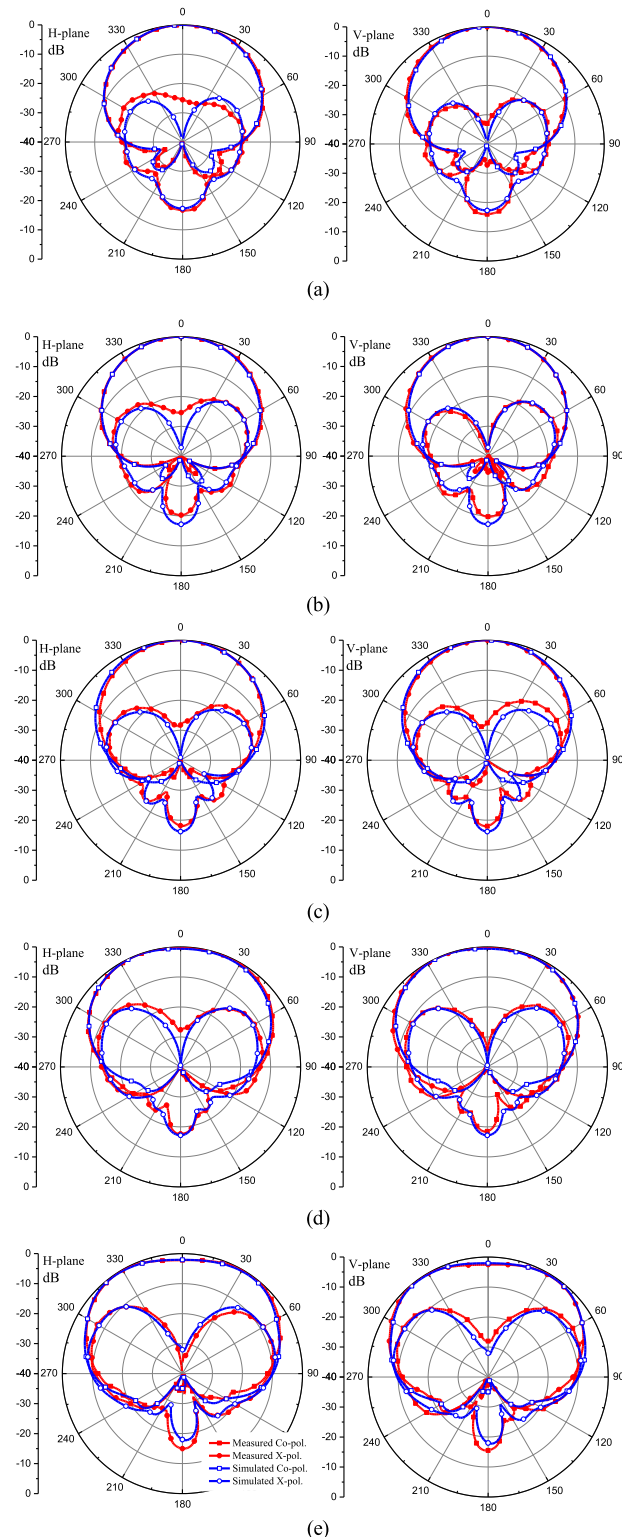


FIGURE 13. Measured and simulated normalized radiation patterns of the proposed antenna. (a) 1.7 GHz. (b) 2.2 GHz. (c) 2.7 GHz. (d) 3.2 GHz. (e) 3.6 GHz.

IV. RESULTS AND DISCUSSION

A prototype of proposed antenna was fabricated and measured. The photographs of the fabricated antenna and its

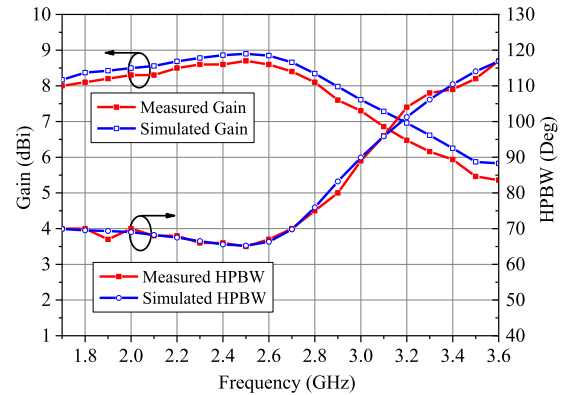


FIGURE 14. Measured and simulated antenna gain and HPBW.

measurement in the anechoic chamber are shown in Fig. 11. The antenna was measured at University of Kent, the UK. Both the simulated and measured VSWR and isolation are provided in Fig. 12 for comparison. The overlapped impedance bandwidth for both ports is 74.5% (from 1.69 GHz to 3.7 GHz) for VSWR < 1.5, which is slightly wider than the simulated results, which is caused by the fabrication tolerance. The VSWR of port 2 is slightly worse than port 1. This is due to the via hole configuration which is used to avoid the intersection, but the VSWR is still good below 1.5. The measured isolation between the two ports is higher than 30 dB over the whole impedance bandwidth, which agrees well with the simulated result.

To illustrate the radiation patterns, the *xz* plane is defined as the H-plane (Horizontal plane) and *yz* plane is defined as the V-plane (Vertical plane). Radiation patterns of both H-plane and V-plane are given in Fig. 13. It can be seen that, because of the symmetry of the antenna, measured radiation patterns of both planes are of great resemblance, and agree well with the simulated results. The measured XPD at the boresight direction is higher than 25 dB for base station communication frequency band (1.7 GHz ~ 2.7 GHz), and the XPD is even better at the remains upper frequency band. Fig. 14 shows the measured and simulated gain and HPBW. The measured HPBW is between 65° and 70° from 1.7 GHz to 2.7 GHz, while the gain is from 8 dBi to 8.7 dBi. The HPBW increases to 117° and the gain decreased to 5.4 dBi at 3.6 GHz.

Table 2 compares the proposed antenna with other recently reported dual-polarized antennas that operate at the similar frequency band. It is found that with a relatively compact size, the impedance bandwidth of the proposed antenna is wider than these reported designs due to the multi-resonance characteristic and the wideband baluns employed in the design. Furthermore, the proposed antenna has very stable radiation characteristic for base station applications. Therefore, there is no need to modify the reflector to stabilize the radiation property, which can decrease the design complexity and cost of the antenna.

TABLE 2. Comparison of the dual-polarized antennas for base station applications.

Antennas	Size (mm×mm×mm)	Bandwidth	Isolation (dB)	Radiation property for base stations		Modification to the reflector
				Gain (dBi)	HPBW (deg)	
[1]	140×140×34	1.7 GHz-2.7 GHz for VSWR<1.5	>25	7.6-8.8	66-70	Yes
[12]	300×145×34.7	1.63 GHz-2.95 GHz for VSWR<1.5	>31	8.2-8.8	Not Given	Yes
[13]	200×134×36	1.7 GHz-2.7 GHz for RL>15 dB	>30	About 8.5	Around 65	Yes
[16]	160×160×28	1.7 GHz -2.73 GHz for RL>10 dB	>38	>9.3	Not Given	No
[17]	150×150×32.5	1.7 GHz-2.9 GHz for VSWR<1.5	>35	7-8.6	Not Given	No
[20]	140×140×34	1.7 GHz-2.9 GHz for VSWR<1.5	>26	About 8.5	63-69	Yes
[28]	160×160×40	1.7 GHz -2.75 GHz for RL>15 dB	>45	About 9	57-73	No
This work	150×150×35	1.7 GHz-3.7 GHz for VSWR<1.5	>30	8-8.7	65-70	No

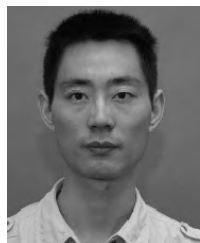
V. CONCLUSION

A wideband dual-polarized antenna using four integrated baluns and shorted dipoles is proposed in this paper. With the symmetrical radiator, the proposed antenna is excited by two crossed feed lines. By using the configuration of the wideband baluns and the crossed feed lines, the proposed antenna exhibits a wideband impedance bandwidth of 74.5% (from 1.7 GHz to 3.7 GHz) for VSWR<1.5 and high isolation (>30 dB) between the two ports over the whole impedance bandwidth. By properly adjusting antenna design parameters, stable gain and HPBW are obtained for base station applications. Measured radiation patterns show that the proposed antenna has a stable gain (from 8.0 dBi to 8.7 dBi) and a stable HPBW (from 65° to 70°) for the upper band (1.7 GHz to 2.7 GHz) base station applications. With the wideband impedance bandwidth and good unidirectional radiation patterns, the application of the proposed dual-polarized antenna is not only limited to the base stations, but also can be applied to other wireless systems such as radars, satellites and other wireless systems.

REFERENCES

- [1] Q.-X. Chu, D.-L. Wen, and Y. Luo, "A Broadband $\pm 45^\circ$ dual-polarized antenna with Y-shaped feeding lines," *IEEE Trans. Antennas Propag.*, vol. 63, no. 2, pp. 483–490, Feb. 2015.
- [2] W. Hong et al., "Multibeam antenna technologies for 5G wireless communications," *IEEE Trans. Antennas Propag.*, vol. 65, no. 12, pp. 6231–6249, Dec. 2017.
- [3] S.-C. Gao, L.-W. Li, M.-S. Leong, and T.-S. Yeo, "Dual-polarized slot-coupled planar antenna with wide bandwidth," *IEEE Trans. Antennas Propag.*, vol. 51, no. 3, pp. 441–448, Mar. 2003.
- [4] S. Gao, L. W. Li, M. S. Leong, and T. S. Yeo, "A broad-band dual-polarized microstrip patch antenna with aperture coupling," *IEEE Trans. Antennas Propag.*, vol. 51, no. 4, pp. 898–900, Apr. 2003.
- [5] H. W. Lai and K. M. Luk, "Dual polarized patch antenna fed by meandering probes," *IEEE Trans. Antennas Propag.*, vol. 55, no. 9, pp. 2625–2627, Sep. 2007.
- [6] Y. Gou, S. Yang, Q. Zhu, and Z. Nie, "A compact dual-polarized double e-shaped patch antenna with high isolation," *IEEE Trans. Antennas Propag.*, vol. 61, no. 8, pp. 4349–4353, Aug. 2013.
- [7] Y.-X. Guo, K.-W. Khoo, and L. C. Ong, "Wideband dual-polarized patch antenna with broadband baluns," *IEEE Trans. Antennas Propag.*, vol. 55, no. 1, pp. 78–83, Jan. 2007.
- [8] H.-W. Son, "Design of dual-polarised microstrip antenna with high isolation using capacitive feeds," *Electron. Lett.*, vol. 45, no. 11, pp. 533–534, May 2009.
- [9] W. Qiu, C. Chen, H. Zhang, and W. Chen, "A wideband dual-polarized L-probe antenna array with hollow structure and modified ground plane for isolation enhancement," *IEEE Antennas Wireless Propag. Lett.*, vol. 16, pp. 2820–2823, 2017.
- [10] C.-X. Mao, S. Gao, Y. Wang, F. Qin, and Q.-X. Chu, "Multimode resonator-fed dual-polarized antenna array with enhanced bandwidth and selectivity," *IEEE Trans. Antennas Propag.*, vol. 63, no. 12, pp. 5492–5499, Dec. 2015.
- [11] C.-X. Mao, S. Gao, Y. Wang, Q. Luo, and Q.-X. Chu, "A shared-aperture dual-band dual-polarized filtering-antenna-array with improved frequency response," *IEEE Trans. Antennas Propag.*, vol. 65, no. 4, pp. 1836–1844, Apr. 2017.
- [12] Z. Bao, Z. Nie, and X. Zong, "A novel broadband dual-polarization antenna utilizing strong mutual coupling," *IEEE Trans. Antennas Propag.*, vol. 62, no. 1, pp. 450–454, Jan. 2014.
- [13] Y. H. Cui, R. L. Li, and H. Z. Fu, "A broadband dual-polarized planar antenna for 2G/3G/LTE base stations," *IEEE Trans. Antennas Propag.*, vol. 62, no. 5, pp. 4836–4840, Sep. 2014.
- [14] Y. Luo, Q.-X. Chu, and D.-L. Wen, "A plus/minus 45 degree dual-polarized base-station antenna with enhanced cross-polarization discrimination via addition of four parasitic elements placed in a square contour," *IEEE Trans. Antennas Propag.*, vol. 64, no. 4, pp. 1514–1519, Apr. 2016.
- [15] D.-L. Wen, D.-Z. Zheng, and Q.-X. Chu, "A dual-polarized planar antenna using four folded dipoles and its array for base stations," *IEEE Trans. Antennas Propag.*, vol. 64, no. 12, pp. 5536–5542, Dec. 2016.
- [16] B. Li, Y.-Z. Yin, W. Hu, Y. Ding, and Y. Zhao, "Wideband dual-polarized patch antenna with low cross polarization and high isolation," *IEEE Antennas Wireless Propag. Lett.*, vol. 11, pp. 427–430, 2012.
- [17] Y. Gou, S. Yang, J. Li, and Z. Nie, "A compact dual-polarized printed dipole antenna with high isolation for wideband base station applications," *IEEE Trans. Antennas Propag.*, vol. 62, no. 8, pp. 4392–4394, Aug. 2014.
- [18] Y. H. Ren, J. Ding, C. J. Guo, Y. Qu, and Y. C. Song, "A wideband dual-polarized printed antenna based on complementary split-ring resonators," *IEEE Antennas Wireless Propag. Lett.*, vol. 14, pp. 410–413, 2015.
- [19] A. Elsherbini, J. Wu, and K. Sarabandi, "Dual polarized wideband directional coupled sectorial loop antennas for radar and mobile base-station applications," *IEEE Trans. Antennas Propag.*, vol. 63, no. 4, pp. 1505–1513, Apr. 2015.
- [20] D.-L. Wen, D.-Z. Dong, and Q.-X. Chu, "A wideband differentially fed dual-polarized antenna with stable radiation pattern for base stations," *IEEE Trans. Antennas Propag.*, vol. 65, no. 5, pp. 2248–2255, May 2017.
- [21] K.-M. Luk and H. Wong, "A new wideband unidirectional antenna element," *Int. J. Microw. Opt. Technol.*, vol. 1, no. 1, pp. 35–44, Jun. 2006.
- [22] B. Q. Wu and K. M. Luk, "A broadband dual-polarized magneto-electric dipole antenna with simple feeds," *IEEE Antennas Wireless Propag. Lett.*, vol. 8, pp. 60–63, 2009.
- [23] H. W. Lai, K. K. So, H. Wong, C. H. Chan, and K. M. Luk, "Magneto-electric dipole antennas with dual open-ended slot excitation," *IEEE Trans. Antennas Propag.*, vol. 64, no. 8, pp. 3338–3346, Aug. 2016.
- [24] F. Zhu et al., "Ultra-wideband dual-polarized patch antenna with four capacitively coupled feeds," *IEEE Trans. Antennas Propag.*, vol. 62, no. 5, pp. 2440–2449, May 2014.
- [25] G. Adamiuk, T. Zwick, and W. Wiesbeck, "Compact, dual-polarized UWB-antenna, embedded in a dielectric," *IEEE Trans. Antennas Propag.*, vol. 58, no. 2, pp. 279–286, Feb. 2010.
- [26] M. Sonkki, D. Sánchez-Escuderos, V. Hovinen, E. T. Salonen, and M. Ferrando-Bataller, "Wideband dual-polarized cross-shaped Vivaldi antenna," *IEEE Trans. Antennas Propag.*, vol. 63, no. 6, pp. 2813–2819, Jun. 2015.

- [27] W. K. Roberts, "A new wide-band balun," *Proc. IRE*, vol. 45, no. 12, pp. 1628–1631, Dec. 1957.
- [28] Y. Cui, X. Gao, and R. Li, "A broadband differentially fed dual-polarized planar antenna," *IEEE Trans. Antennas Propag.*, vol. 65, no. 6, pp. 3231–3234, Jun. 2017.
- [29] H. Sun, C. Ding, B. Jones, and Y. J. Guo, "A wideband base station antenna element with stable radiation pattern and reduced beam squint," *IEEE Access*, vol. 5, pp. 23022–23031, 2017.



LE-HU WEN received the M.S. degree from Xidian University, Xi'an, China, in 2011. He is currently pursuing the Ph.D. degree with the University of Kent, Canterbury. His current research interests include multi-band base station antenna, mobile terminal antenna, and tightly coupled array.



STEVEN GAO (M'01–SM'16) is currently a Professor and the Chair of RF and microwave engineering with the University of Kent, U.K. He has authored two books including the *Space Antenna Handbook* (Wiley, 2012) and the *Circularly Polarized Antennas* (IEEE Wiley, 2014), over 200 papers, and several patents. His research covers smart antennas, phased arrays, multi-in multi-out, satellite antennas, RF/microwave/mm-wave circuits, satellite communications, ultra-wideband radars, synthetic-aperture radars, and mobile communications. He is a Distinguished Lecturer of the IEEE AP-S, an Associate Editor of the *IEEE TRANSACTIONS ON ANTENNAS AND PROPAGATION* and the *Radio Science*, and the Editor-in-Chief of Wiley Book Series on Microwave and Wireless Technologies. He was the General Chair of LAPC 2013 and a Keynote Speaker or Invited Speaker at some international conferences, such as AES'2014 (China), IWAT'2014 (Sydney), SOMIRES'2013 (Japan), and APCAP'2014 (China).



CHUN-XU MAO was born in Hezhou, China. He received the M.S. degree in RF and microwave engineering from the South China University of Technology in 2013 and the Ph.D. degree from the University of Kent, U.K., in 2017. He is currently a Post-Doctoral Research Associate with the Computational Electromagnetics and Antennas Research Laboratory, Department of Electrical Engineering, Pennsylvania State University, USA. His research interests include filtering antenna integration, ultra-wideband antenna, circularly polarized satellite antenna array, multiband synthetic aperture radar antenna array, multifunctional RF frontend, and wearable antenna.



QI LUO (S'08–M'12) received the M.Sc. degree in data communications from The University of Sheffield, Sheffield, U.K., in 2006, and the Ph.D. degree in electrical engineering from the University of Porto, Porto, Portugal, in 2012. From 2012 to 2013, he was a Research Fellow with the Surrey Space Center, Guildford, U.K. He is currently a Research Associate with the School of Engineering and Digital Arts, University of Kent, Canterbury, U.K. His current research interests include smart antennas, circularly polarized antennas, reflectarray, multiband microstrip antennas, and electrically small antenna design. He has been serving as a reviewer for a number of technical journals and conferences. He is an Outstanding Reviewer for the *IEEE TRANSACTIONS ON ANTENNAS AND PROPAGATION* in 2015.



WEI HU (S'09–M'14) received the B.S. degree in electronic information engineering and the Ph.D. degree in electromagnetic fields and microwave technology from Xidian University, Xi'an, China, in 2008 and 2013, respectively. He is currently an Associate Professor with the National Key Laboratory of Antennas and Microwave Technology, Xidian University. His current research interests include multiband and wideband antennas, circularly polarized and dual-polarized antennas, and multi-in multi-out technologies.



YINGZENG YIN received the B.S., M.S., and Ph.D. degrees in electromagnetic wave and microwave technology from Xidian University, Xi'an, China, in 1987, 1990, and 2002, respectively. From 1990 to 1992, he was a Research Assistant and an Instructor with the Institute of Antennas and Electromagnetic Scattering, Xidian University, where he was an Associate Professor with the Department of Electromagnetic Engineering from 1992 to 1996 and has been a Professor since 2004. His current research interests include the design of microstrip antennas, feeds for parabolic reflectors, artificial magnetic conductors, phased array antennas, and computer aided design for antennas.



XUEXIA YANG (S'98–A'01–M'02–SM'17) received the B.S. and M.S. degrees from Lanzhou University, Lanzhou, China, in 1991 and 1994, respectively, and the Ph.D. degree in electric engineering from Shanghai University, Shanghai, China, in 2001. From 1994 to 1998, she was a Teaching Assistant and a Lecturer with Lanzhou University. From 2001 to 2008, she was a Lecturer and an Associate Professor with Shanghai University, where she is currently a Professor and the Head of the Antennas and Microwave Research and Development Center. She is a member of the Committee of Antenna Society, China Electronics Institute, and a Senior Member of the China Electronics Institute.